Terahertz Subsurface Imaging System

E. Nova, J. Abril, M. Guardiola, S. Capdevila, A. Broquetas, J. Romeu, L. Jofre,
AntennaLab, Signal Theory and Communications Dpt.
Universitat Politècnica de Catalunya
Jordi Girona 1-3, Barcelona, 08043, Spain
{romeu, enrique.nova}@tsc.upc.edu

***Abstract*— A subsurface imaging system based on a terahertz time-domain spectrometer (THz-TDS) is described in this paper. The system performance has been simulated in terms of spatial resolution, penetration capabilities and SNR. Moreover, a commercial THz-TDS has been used to perform the proof-of-concept of the described system.**

I. Introduction

Terahertz imaging systems are gaining relevance in the field of electromagnetic imaging thanks to their good compromise between spatial resolution and penetration capabilities. The inherent available large bandwidth and the specific spectral absorption behavior of certain molecules are key elements in defining the potentialities of such systems. Moreover, the recent evolution of electromagnetic sources working at this frequency band opens a new scope of applications to be developed using terahertz radiation. Since most non-polar, non-metallic materials are relatively transparent to terahertz radiation, non destructive testing can be performed through their surfaces. Furthermore, the available terahertz time domain spectroscopy systems emit narrow pulses with large spectral content approximately from 0.3 THz to 3 THz. Hence, these systems are well suited to perform subsurface imaging since they can yield depth resolutions in the order of few micrometers.

In the next sections, a subsurface imaging setup based on a THz-TDS system is proposed and simulated in order to foresee its performance. Furthermore, in order to validate the simulations a set of measurements have been performed using a commercial THz spectrometer.

II. Setup Geometry

Fig.1 shows the proposed system diagram [1] based on a terahertz time-domain spectroscopy system. In this scheme, the measurements are done in reflection. Terahertz radiation is created at the transmitting photoconductive antenna (Tx PCA), collimated by a mirror and aimed to the sample. The reflected scattered fields produced by the incident beam are guided towards a retina using a beamsplitter.

The retina is able to recover the value of electric field at the position of each element using the modulated scatterer technique (MST) [2].

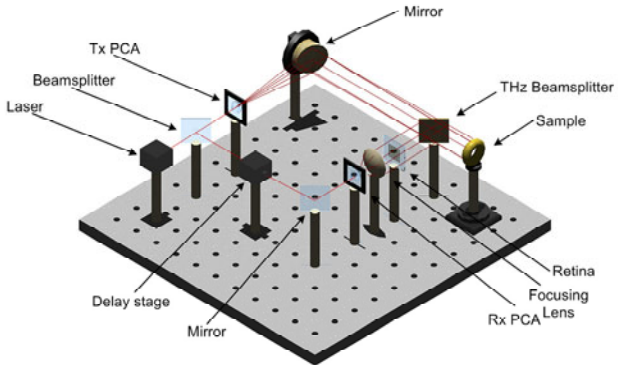

Fig.1: THz subsurface imaging system

In Fig.2, the design of the retina is presented. It is composed by 8x8 UWB elements. A Nano Electromechanical System (NEMS) [3] is placed at the center of each element, changing its load status depending on the NEMS state. Hence, using the variation of the element load status, the field can be modulated at its position and therefore measured using the MST technique.

Once the electric field has crossed the retina, it is focused onto the receiving photoconductive antenna (Rx PCA) using a lens. A probe pulse is taken from the source laser and delayed using a controllable mechanical delay stage. The sampling of the terahertz electric field at the receiving antenna is controlled by the probe pulse, enabling a coherent detection of the incident THz radiation. Finally, the current created at the Rx PCA is amplified using a lock-in amplifier and processed using the FFT to obtain the spectral content of the pulse.

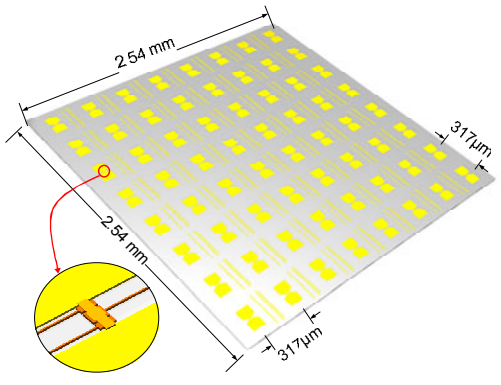

Fig.2: Retina layout and dimensions

III. Simulation Results

In order to predict the performance of the system, simulations of the image reconstruction algorithm have been carried out. Once the field distribution along the retina is known, a focusing algorithm is applied to reconstruct a transversal image. The simulations have been performed using an FDTD electromagnetic simulator [4]. A 16x16 array of probes spaced λ/2 at 1 THz have been used to recover the field at 2 mm from the object. A Gaussian pulse with spectral content from 500 GHz to 1.5 THz has been used as excitation. The equation (1) has been applied to focus the field, where $\tilde{\psi}(x,y)$ is a reconstructed image pixel, $E(x',y';f)$ is the electric field value at the probe placed at coordinates (x',y') and $r_{x,y}(x',y')$ is the distance from the probe to the pixel.

$$\tilde{\psi}(x,y) = \sum_{f}\sum_{x',y'} E(x',y';f)\cdot e^{jk\cdot r_{x,y}(x',y')} \qquad (1)$$

Fig. 3 shows the results of the simulation of a perfect electric conductor (PEC) block of 2x2 mm. The shape of the object is perfectly recovered. Moreover, the existence of a crack on the surface can be also exposed.

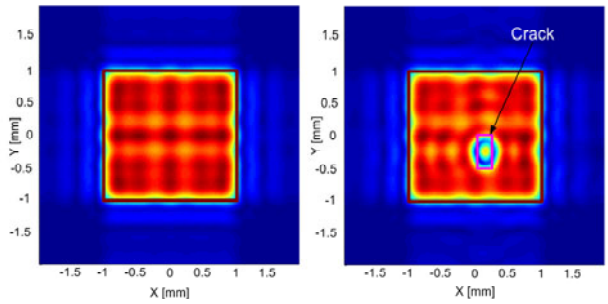

(a) (b)

Fig.3: Reconstructed image from a PEC block of 2x2 mm (a). In (b), a crack of 0.2x0.5x0.3 mm has been added to the block simulated in (a).

Spectral imaging simulations have been also carried out. A strip of lossy dielectric material of 0.4x1 mm has been inserted into a lossless dielectric block of 1x1 mm. The permittivity value for both materials is ε_r=4, however the strip material has an absorption peak at 1 THz with a complex permittivity of ε_r=4+j9 at this frequency. Fig. 4 (a) shows the results of a simulation using the full excitation bandwidth whereas in Fig. 4(b) only a frequency band from 975 GHz to 1025 GHz is used to reconstruct the image. The strip can be revealed when a narrow bandwidth around the strip absorption frequency is used. Furthermore a complete spectral response of each pixel can be obtained.

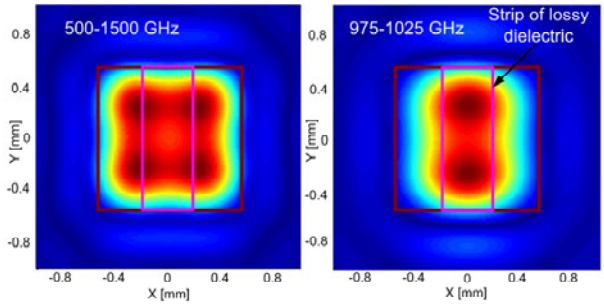

(a) (b)

Fig.4: Image reconstruction of a lossy dielectric embedded in a lossless block. (a) presents a complete reconstruction using the full bandwidth, (b) shows the reconstruction using only information around the peak absorption band.

IV. Setup Characterization

The SNR at the receiver has been characterized for different values of the sample dielectric permittivity. A source power of 20 μW and a 15% of coupling efficiency have been considered [5]. Thus, a beam power of 3 μW can be obtained. The multiplexing losses due to the retina are 18 dB whereas the losses due to the field modulation have been considered 6 dB. The noise current at the receiving photoconductive antenna is $1.3\cdot10^{-13}$ A rms. The losses due to atmospheric absorption and retina absorption have been neglected in front of the multiplexing losses. With these values, the achieved SNR curves for permittivity values of ε_r=40, ε_r=20 and ε_r=5 are depicted against total integration time for the 8x8 element retina in Fig. 5.

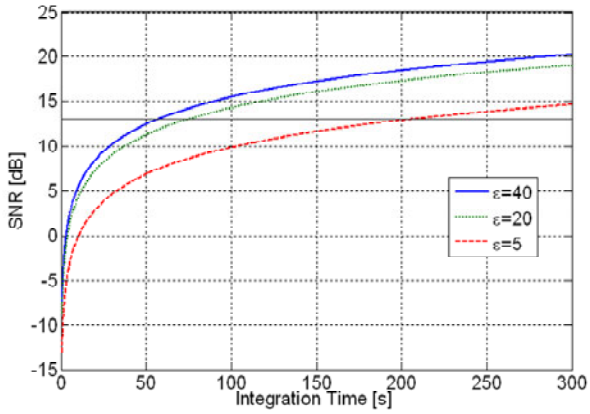

Fig.5: Achieved SNR against integration time for different sample dielectric constants

The minimum required value of SNR necessary to obtain an image has been considered 13 dB. Hence, the integration time needed to reconstruct the full image will be 57 s, 75 s and 206 s for ε_r=40, ε_r=20 and ε_r=5 respectively.

V. MEASUREMENTS

A. Measurement setup

A portable THz-TDS system [6] has been used to obtain raster images in reflection. This spectrometer allows to measure in real time with a dynamic range of around 25 dB and a repetition rate greater than 7 Hz. Nevertheless, the aforementioned value of dynamic range can be improved if the measurement is averaged for several acquisitions.

The transmitted pulse has approximately 2.5 THz of bandwidth. Therefore a depth resolution of about 60 µm is achieved when measuring in reflection. Fig. 6 shows the setup geometry used to obtain the images presented in this section. The spectrometer is fixed on an optical breadboard whereas the sample is held on a 3D stage composed of three independent linear stages. Using the linear stage in Z direction, the sample can be placed at the focus of the lens where the measured beam waist is 170 µm; therefore at this Z position a pixel resolution of 340 µm is obtained.

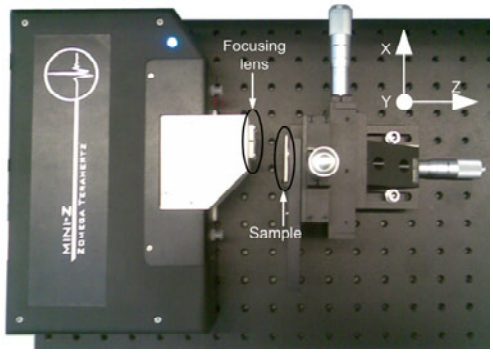

Fig.6: Photograph of the measurement setup

The raster imaging is performed by displacing the sample in X and Y directions every pixel resolution distance. In the case of this paper, the image pixels have been measured moving the sample every 254 µm, below the spatial resolution.

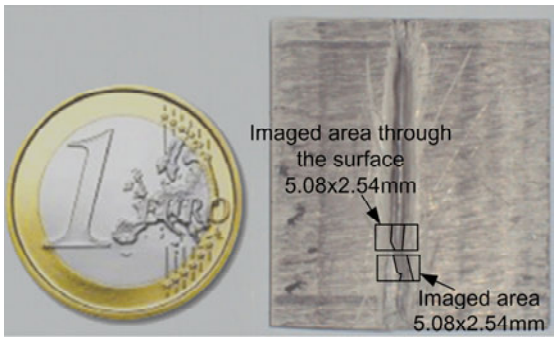

Fig.7: Photograph of the measured sample. Both imaged areas are illustrated on the photograph.

Fig. 7 shows the sample of ceramic dielectric material of relative permittivity ε_r= 13 (measured in X-band) used to perform the imaging. The dimensions of the sample are 29x33 mm and it has a thickness of 2.4 mm. A crack of approximately 2 mm of width has been cut on the surface with a depth of around 0.5 mm.

Two types of images have been obtained. First a surface image that gives information about the shape of the sample face in front of the lens has been retrieved. This image has been reconstructed by using the first reflection of the transmitted pulse. The second type of acquired image gives information about the shape of the opposite face of the sample. The second reflection of the transmitted pulse has been used to process the latter image.

Both measured areas are shown in Fig. 7, where the shape profile has been depicted to better understand the images of the following section.

B. Measurements analysis

In this section an analysis of the obtained measurements and images is carried out. Fig. 8 shows two reflected signals in temporal domain from two different pixel positions when looking at the front face. The blue line corresponds to a reflection of a surface pixel. The time reference has been taken on the maximum of this reflection. The green dotted line of the same graph shows the signal reflected on the crack. The latter is delayed by 3.5 ps, agreeing with a crack depth on the order of 0.5 mm. Furthermore, a significant reduction on the amplitude is observed between two reflections due to the scattering produced by the irregular shape of the crack.

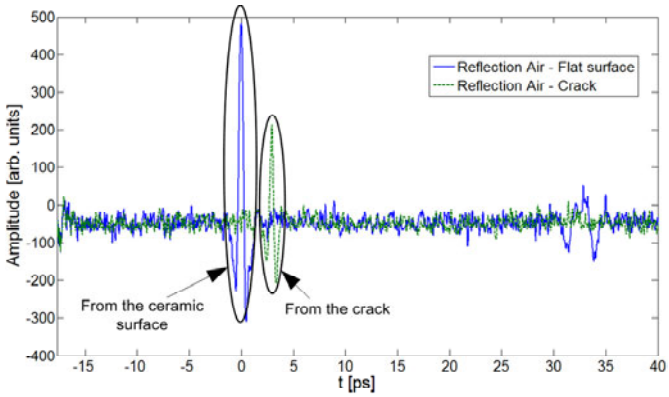

Fig.8: Reflected signals from a pixel on the surface of the sample and from a pixel on the crack (blue and green lines respectively).

Two images have been reconstructed using 20x10 pixel measurements. It has to be pointed out that the images have been interpolated in order to improve the perception of the shapes. Fig. 9 shows the surface shape of the sample around the crack, in the area depicted in Fig. 7. The processing of this image is based on taking the amplitude value at a fixed delay. In this case, to form the image the delay is 0. The contour shape of the crack is recovered, however the transitions are attenuated.

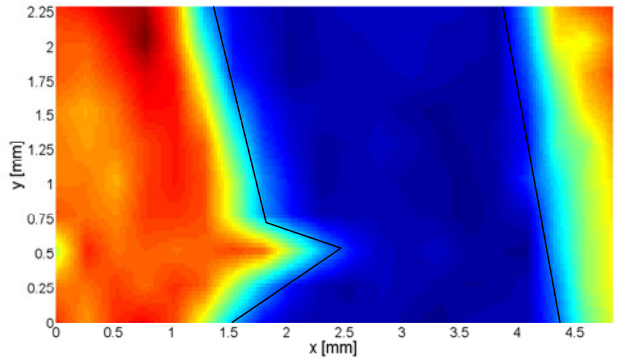

Fig.9: Image obtained when focusing to the surface of the sample

The Fig. 10 shows an image of the same area as Fig. 9 but in this case 3.5 ps of time delay has been used to retrieve the image. With this delay the picture gives information about the inner contour of the crack. This contour matches with the depicted crack shape of Fig. 7.

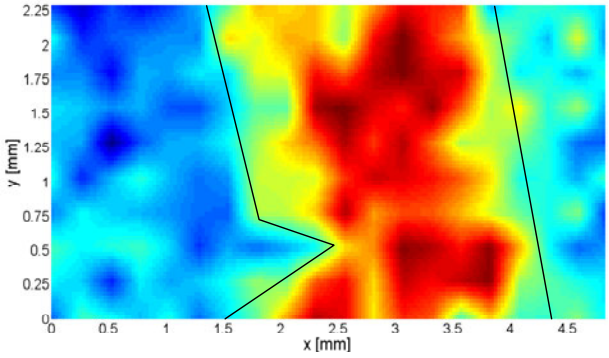

Fig.10: Image obtained when focusing to the crack on the opposite face

Fig. 10 uses the reflection between the sample material and the air at the opposite face in order to form the image. Fig. 11 shows the signal reflected in the transition from the surface to air in blue colour, whereas the signal reflected in the transition from the crack to the air is depicted in green. The time reference has been taken on the surface of the sample. A delay of 16 ps exists between both reflections. Using the relative permittivity of the material this delay is translated to 0.6 mm of crack depth.

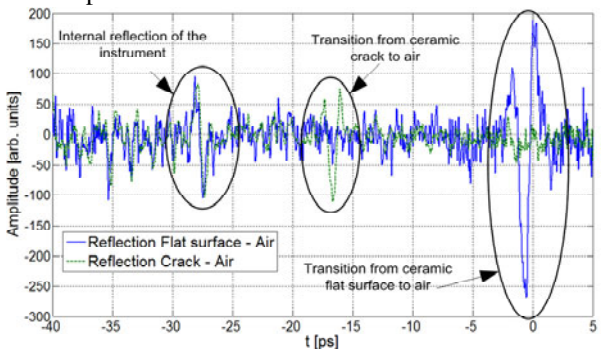

Fig.11: Reflected signals from a pixel on the opposite face of the sample and from a pixel on the crack (blue and green lines respectively).

Fig. 12 shows the reconstruction of the image using a time delay of 0. The shape of the surface in the opposite face is recovered. Now it has to be pointed out that the variations in the surface are better observed since the depth resolution is improved by a factor of $\sqrt{\varepsilon_r}$. Moreover the effect of the transitions becomes more noticeable.

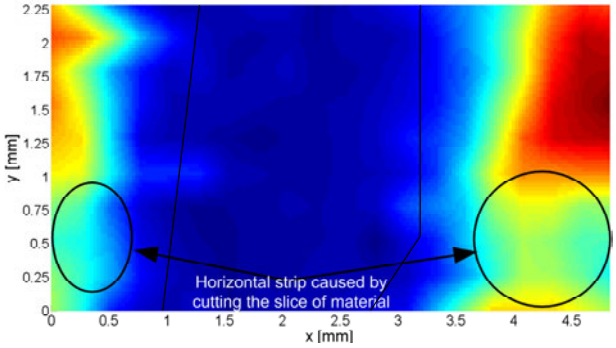

Fig.12: Image obtained when focusing to opposite face

Fig. 13 shows a reconstruction of the measured pixels when the delay applied is -16 ps. The crack shape is recovered. As in Fig. 12, the effect of the transitions is increased and only the stable surface of the crack is retrieved. This image proves the penetration capabilities of the terahertz radiation, being capable of penetrate 2.5 mm of high permittivity material with around 14 dB SNR averaging during 6 seconds. A full subsurface image of 20x10 pixels can be ideally recovered with this system in 20 minutes.

However, the measured pixels to obtain Fig. 9 and Fig. 10 have been averaged for 1 second, leading a measuring time of 200 s. This value is in accordance with the results presented in Fig. 5.

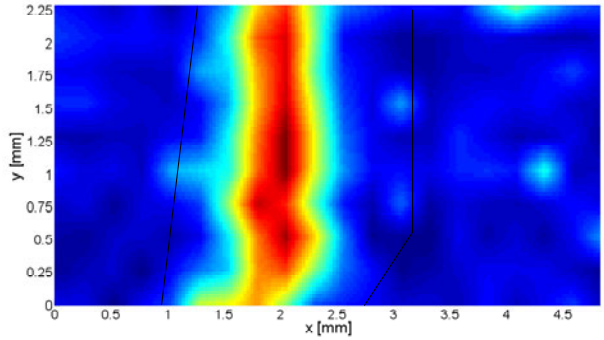

Fig.13: Image obtained when focusing to the crack on the opposite face

VI. Conclusions

A system based on a terahertz time-domain spectroscopy and capable of perform subsurface imaging in reflection using a retina has been proposed. Preliminary simulations have been carried out in order to show the imaging capabilities of the system. Moreover, a first calculation of the SNR of the system has been performed to foresee the acquisition time needed to form an image. The proof-of-concept of our system proposal

has been carried out using a commercial THz-TDS spectrometer. This system has been used to acquire images through a ceramic material, revealing the existence of a crack on the opposite face, and proving the penetration capabilities of the terahertz radiation.

ACKNOWLEDGMENT

We are grateful to Albert Redó, Gerard Salvatella and Regina Galceran from the *Universitat de Barcelona* for the received support on the utilization of the terahertz spectrometer.

This work was supported in part by Spanish CICYT under projects TEC2004-04866-C04-02 and TEC2007-66698-C04-01 and CONSOLIDER CSD2008-68.

REFERENCES

[1] E. Nova, J. Abril, M. Guardiola, S. Capdevila, A. Broquetas, J. Romeu, L. Jofre, *Terahertz Tomographic Imaging Technologies*, Proceedings of URSI-Spain 2009

[2] Bolomey, J. and Gardiol, F. E., *Engineering Applications of the Modulated Scatterer Technique*, Artech House, 2001

[3] Bedri A. Cetiner, Necmi Biyikli, *Penta-Band Planar Inverted F-Antenna (PIFA) Integrated by RF-NEMS Switches,* UGIM 2008

[4] Steven G. Johnson and John D. Joannopoulos, *MEEP freely available FDTD simulation software*, Massachusetts Institute of Technology

[5] Martin van Exter and Daniel R. Grischkowsky, *Characterization of an Optoelectronic Terahertz Beam System*, IEEE Trans. on Microwave Theory and Techniques, vol. 38, no. 11, 1990

[6] *Mini-Z terahertz time-domain spectrometer, Zomega corp., 2010*